Journal of Engineering Science and Technology
Vol. 6, No. 6 (2011) 769 - 776

PERFORMANCE OPTIMIZATION OF LINEAR INDUCTION MOTOR BY EDDY CURRENT AND FLUX DENSITY DISTRIBUTION ANALYSIS

M. S. MANNA[1], S. MARWAHA[1,*], A. MARWAHA[2]

[1]Electrical & Instrumentation Engineering Department, Faculty of Engineering,
[2]Electronics and Communication Engineering Department, Faculty of Engineering,
Sant Longowal Institute of Engineering & Technology, Longowal Punjab, India
*Corresponding Author: marwaha_sanjay@yahoo.co.in

Abstract

The development of electromagnetic devices as machines, transformers, heating devices confronts the engineers with several problems. For the design of an optimized geometry and the prediction of the operational behaviour an accurate knowledge of the dependencies of the field quantities inside the magnetic circuits is necessary. This paper provides the eddy current and core flux density distribution analysis in linear induction motor. Magnetic flux in the air gap of the linear induction motor (LIM) is reduced to various losses such as end effects, fringes, effect, skin effects etc. The finite element based software package COMSOL Multiphysics Inc. USA is used to get the reliable and accurate computational results for optimization the performance of LIM. The geometrical characteristics of LIM are varied to find the optimal point of thrust and minimum flux leakage during static and dynamic conditions.

Keywords: Linear induction motor, Finite element method, Eddy current, Flux density distribution.

.

1. Introduction

Electromagnetic field analysis of electromechanical devices is usually performed to achieve information about their stationary and dynamic performances. In many applications, a two-dimensional finite element analysis ables to predict with sufficient approximation device performances. Unfortunately, some core struc-tures or some behaviour conditions cannot be simulated by an equivalent 2D domain and

Nomenclatures

$\vec{A}$	Magnetic vector potential, Vs/m
$\vec{B}$	Magnetic flux vector, T
B_x, B_y	Magnetic flux density in *x*,*y* direction, T
E_z	Electric field in *z*-direction, V/m
F	Force, N
F_n	Force in the normal direction, N
F_x	Force in the *x*-axis direction, N
G	Goodness factor
g	Air gap between primary and secondary stacks, mm
H	Magnetic Intensity, AT/m
H_y	Magnetic Intensity in *y*-direction, AT/m
I_1	Current in primary sheet, A
J	Surface current density, A/m
J_o	Primary surface current density, A/m
$\vec{J}_o$	Primary vector surface current density, A/m
K_c	Correction factor
k_ω	Winding factor
l	Length of mover, mm
P	Number of poles
r	Primary/mover notation
S	Secondary notation
t	Time, s
$\vec{v}$	Velocity vector, m/s
w	Primary stack width, mm

Greek Symbols

β	Chording factor
μ	Permeability, N/A^2
μ_o	Absolute permeability, N/A^2
σ	Conductivity, S/m
τ	Pole pitch, mm
ω	Number of turns
ω_1	Number of primary turns

Abbreviations

DOF	Degree of Freedom
FEM	Finite Element Method
LIM	Linear Induction Motor

only a 3D FE analysis provides and accurate model of the electromagnetic problem.

In particular one of the main problems usually encountered in the analysis of linear induction motor is represented by end effects. The eddy currents induced in

the conducting plate create a counter mmf which opposes the passage of the slot leakage flux. Thus the leakage reactance of the linear motor is decreased and more flux is concentrated in air gap, resulting in an increase of the developed thrust. This paper presents the eddy current and secondary core flux density distribution of smaller size LIM.

2. Linear Induction Motor Model

The two dimensional finite element analysis model of LIM has been designed with following specifications [1]. The geometrical view is shown in Fig. 1.

Number of phases: 3, number of poles: 3

Length of primary stack: 240 mm

Width of magnet: 14 mm

Length of mover: 170 mm

Height of mover: 45 mm,

Height of permanent magnet teeth: 4 mm

Thickness of back-iron: 10 mm

Air gap length: varied from 0.5 mm to 3.5 mm

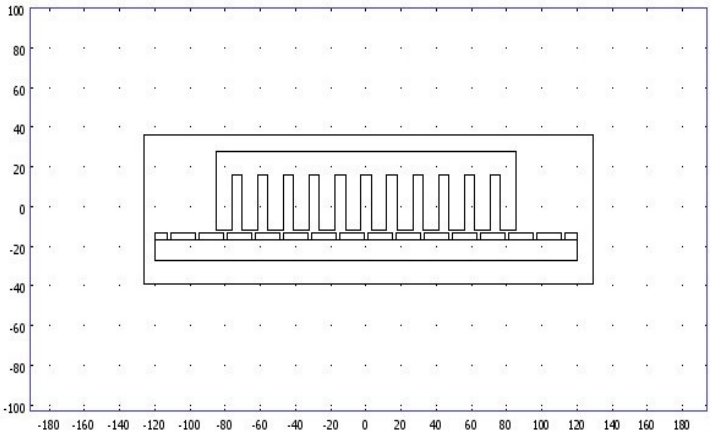

Fig. 1. Geometry Overview of LIM.

The analysis of an LIM is carried out in terms of electromagnetic field equations. As we are well aware that the slotted primary structure with its winding is by no means an ideal boundary conditions, or even a sufficiently simple one. Where, the solution to the governing field equations can be obtained. To reduce the boundary value problem the actual slotted structure is replaced with smooth surface and the current carrying windings are replaced by fictitious, infinitely thin current elements called current sheets, having linear current densities (A/m). The current density distribution of the current sheet is the same as that of the slot-embedded conductor configurations, such that the field in the air gap remains unchanged.

The relationship between the primary current sheet and the resulting air gap field is given by the air gap field equations as given

$$H'_y = H_y + \frac{\partial H_y}{\partial x}\Delta x$$

and

$$E'_z = E_z + \frac{\partial E_z}{\partial x}\Delta x$$

Ampere's law

$$\oint Hdl = \int_S JdS$$

we get

$$g\frac{\partial H_y}{\partial x} = J^S + J^Y$$

$$\frac{\partial E_z}{\partial x} = \mu_o \frac{\partial H_y}{\partial t}$$

$$J^Y = \sigma E_z$$

$$g\frac{\partial^2 H_y}{\partial x^2} = \mu_o \sigma \frac{\partial H_y}{\partial x} + \frac{\partial J^S}{\partial x}$$

In terms of B_y

$$\frac{\partial^2 B_y}{\partial x^2} - \frac{\mu_o \sigma}{g}\frac{\partial B_y}{\partial t} = \frac{\mu_o}{g}\frac{\partial J^S}{\partial x}$$

The governing equation which describes the magnetic vector potential in a single sided linear induction motor is given by

$$rot\frac{1}{\mu} rot\vec{A} = \vec{J}_o - \sigma\left(\frac{\partial \vec{A}}{\partial t} - \vec{v}\times\vec{B}\right) \quad (1)$$

where σ is an equivalent conductivity of mover's material taking account of transverse edge effect [2] and v is the velocity of mover. The current density of the sheet at the primary surfaces is denoted by $\vec{J}_o$. The current sheet distribution is given by

$$\vec{J}_o = J_o e^{j(\omega t - kx)} \quad (2)$$

J_o is related to primary current which is given by

$$J_o = \frac{3\sqrt{2}\omega_1 k_\omega I_1}{P\tau} \quad (3)$$

where ω_1 is the number of turns, k_w is the primary winding factor, τ is the pole pitch and P is the number of poles.

And from above relations the Goodness factor could achieve as

$$G = \frac{\omega \sigma \mu_o}{g\beta^2} \tag{4}$$

From Eq. (4) further computation of force acting on machine could be derived [3]

$$F_x = \int_l^0 \frac{\omega}{2\mu_o} \left\{ \left(B_x^2 - B_y^2\right) n_x + 2 n_y B_x B_y \right\} dl \tag{5}$$

$$F_n = \int_l^0 \frac{\omega}{2\mu_o} \left\{ \left(B_y^2 - B_x^2\right) n_y + 2 n_x B_x B_y \right\} dl \tag{6}$$

where n_x and n_y are the unit normal direction vectors, ω is the primary stack width. In order to improve accuracy, the LIM has been computed at different air gaps and it was observed that entry-end-effect could be reduced to high extent with change in the air-gap by keeping the speed of LIM at constant value of 36 m/s.

3. Finite Element Analysis

Magnetic flux density and eddy current density distribution of the LIM model under consideration has been computed by using FEM based package. Type of elements are used is Lagrange linear. The refined mesh shown in Fig. 2 consists of 4644 elements with 2356 degree of freedom (DOF). The number of boundary elements are 672 and number of vertex elements are 140.

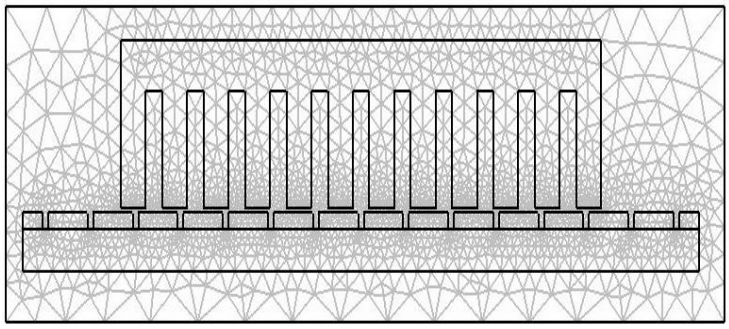

Fig. 2. Meshing of LIM with Adaptive Refinement.

4. Simulation Results

The Drichlet boundary condition on LIM model has been employed. The surface plot obtained for magnetic flux distribution is shown in Fig. 3. The magnetic flux density of secondary core has been analyzed along the motor length during the velocity of 36 m/s of motor. The entry end the magnetic field is weakened by the entry end effect. The field is builds up gradually and rises sharply near the exist end.

Figure 4 shows the fringe effect clearly with magnetization contour. The fringes are more built up at the center of mover core as compared to the both end sides of LIM.

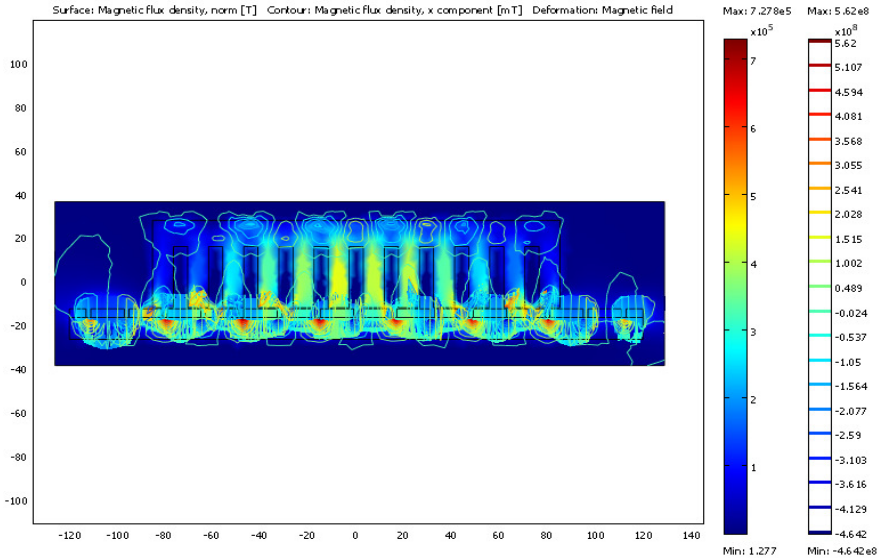

Fig. 3. Magnetic Flux Density Distribution in LIM.

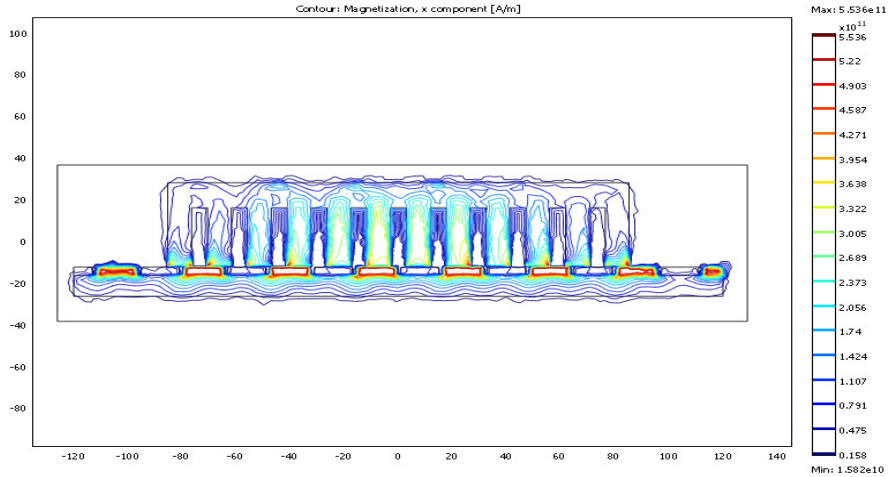

Fig. 4. Magnetisation Contours of LIM.

The surface current density plot is shown in Fig. 5, from which it can be seen that eddy current are more when flux concentration is strong. On the other hand the leakage reactance of the LIM is decreased and more flux is concentrated into the air gap resulting in an increase of the developed thrust. The Simulation results with different air-gap from 0.5 mm to 3.5 mm have been computed and compared. It is found that the optimization in performance achieved of LIM where the air gap is 1 mm between the mover and stator, while the relative permeability is fixed in between 1.0345 to 1.5. The material properties have been kept constant purposely to observe the performance of LIM with geometrical characteristics.

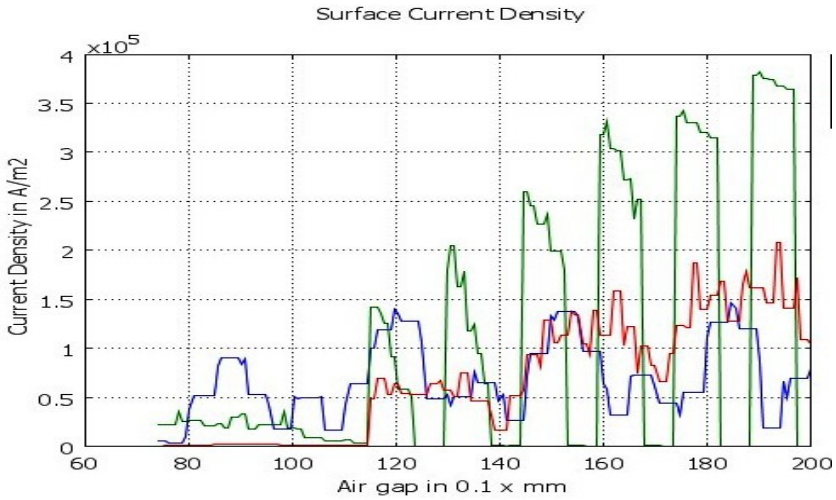

Fig. 5. Surface Current Density at LIM Parts with Different Air Gaps.

5. Effect of Air Gap

The effect of LIM geometry was analysed by many researchers [4-11]. For each geometrical change of the LIM, the tooth eddy loss was calculated by finite element method and compared by analytical method [12, 13]. The ratios of these two analytic and computed losses were termed as correction factor 'K_c' of the given model. It has been noticed here that the correction factor is a function of slot pitch, back plate thickness and most significantly the air gap between primary and secondary of the LIM as shown in Fig. 6.

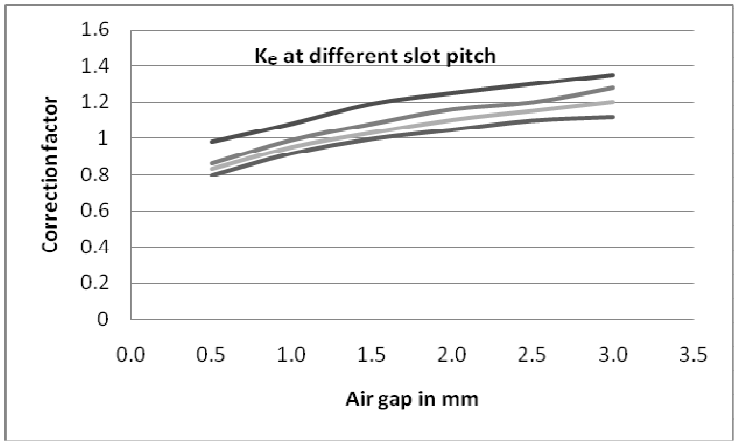

Fig. 6. Correction Factor for Different Geomatry Conditions of LIM.

6. Conclusions

The performance of LIM can be improved by variation in parameters like geometry characteristics, winding structure, material properties. In this paper the attempt has

been made to optimize the performance of LIM by varying the air gap of LIM, whereas other parameters can also be vary to bring optimized model of LIM.

References

1. Roy, D.; Saruhashi, D.; Yamada, S.; and Iwahara, M. (2000). Fabrication and development of a novel flux-concentration type linear induction motor. *IEEE Transactions of Magnetics*, 36(5), 3555-3557.
2. Manna, M.S.; Marwaha, S.; and Marwaha A (2008). Eddy currents analysis of induction motor by 3D FEM. *IEEE Trans. on POWERCON*-08, 1-4.
3. Boldea, I.; and Nasar, S.A. (1985). *Linear motion electromagnetic systems*. John Wiley & Sons Inc., New York.
4. Manna, M.S.; Marwaha, S.; and Vasudeva, C. (2008). Finite element method as an aid to machine design: the state of art. *Proceedings of National Conference on RAEE*, C-2.
5. Fetcher, J.; Williams, B.; and Mahmoud, M. (2005). Air gap flux fringing reduction in inductors using open-circuit copper screens. *IEE proceedings 2005.*
6. Manna, M.S.; Marwaha, S.; and Marwaha, A. (2006). 3D FEM computation and analysis of EM force for electrical rotating machines using FEM. *IEEE Proceedings of PEDES*-06 *International Conference on Power and Electronics, Drives and Energy Systems for Industrial Growth*.
7. Manna, M.S.; Marwaha, S.; Marwaha, A.; and Vasudeva, C. (2009). Two-dimensional quasi-static magnetic field analysis of SLIM using adaptive finite element method. *International Journal in Recent Trends in Engineering*, 2(6), 50-52.
8. Manna, M.S.; Marwaha, S.; Marwaha A.; and Vasudeva, C. (2009). Analysis of permanent magnet linear induction motor (PMLIM) using finite element method. In *International Conference on Advances in Recent Technologies in Communication and Computing, ARTCOM*, 540-542.
9. Rodger, D.; Coles, P.C.; Allen, N.; Lai, H.C.; Leonard, P.J.; and Roberts P. (1997). 3D finite element model of a disc induction machine. *Proceedings of IEE- EMD* 97, 148-149.
10. Yahiaoui, A.; and Bouillant, F. (1994). 2D and 3D numerical computation of electrical parameters of an induction motor. *IEEE Transactions on Magnetics*, 30(5), 3690-3692.
11. Vasudeva, C.; Marwaha, S.; Marwaha, A.; and Manna, M.S. (2010). Air gap effects on magnetic flux density of linear induction motor. *International Journal of Engineering and Information Technology, IJEIT*, 2(1), 37-40.
12. Hairik, A.H.; and Hassan, H.M. (2009). Dynamic model of linear induction motor considering the end effects. *Iraq Journal of Electrical & Electronic Engineering*, 5(1), 38-50.
13. Kumar, A.; Marwaha, S.; Marwaha, A. (2010). Mechanical dynamics analysis of PM generator using h-adaptive refinement. *Journal of Engineering Science & Technology, JESTEC*, 5(1), 41-50.